LAWRENCE
LIVERMORE
NATIONAL
LABORATORY

UCRL-PROC-222446

A multiphase model for heterogeneous explosives in both the dense and dilute limits

D. E. Stevens, M. J. Murphy, T. A. Dunn

June 27, 2006

International Detonation Symposium
Norfolk, VA, United States
July 23, 2006 through July 28, 2006

A MULTIPHASE MODEL FOR HETEROGENOUS EXPLOSIVES IN BOTH THE DENSE AND DILUTE LIMITS

David E. Stevens*, Michael J. Murphy*, Timothy A. Dunn*

*Lawrence Livermore National Laboratory
8000 East Avenue, L-98
Livermore, California, 94551

Abstract. Multiphase flow phenomena are important in the characterization of many particle-loaded explosives. A numerical model of these flows must often be capable of accurately simulating both dense and dilute particle loadings and often the transition between the two limits. This presents severe numerical difficulties in that numerical approaches for packed particle beds often behave poorly for the dilute regime and the reverse is often true for methods developed for the dilute regime. This abstract compares two established numerical methods and presents improvements to them. The improved methods have enabled the development of a general purpose model that has been successfully applied to a wide range of problems including the energetic dispersal of solid particles.

INTRODUCTION

The knowledge of multiphase flow phenomena is crucial to the understanding of many non-ideal explosives. These explosives are characterized by large reaction zones and non-adiabatic processes that invalidate many of the assumptions that go into most current computational tools. The complex behavior of these heterogeneous materials has severely limited the ability to understand their behavior via simulation. Recent advances in Riemann solvers and other methods are now enabling their study without analytic reduction to simpler models that may involve dubious assumptions.

This paper presents two fundamental types of Riemann solvers that are integrated into a single multiphase framework. First we describe the Eulerian-Eulerian particle fluid model for multiphase flow. The numerical method is presented next followed by results and conclusions.

MULTIPHASE FLOW

The Eulerian-Eulerian multiphase formulation is presented in Chinnayya et. al (2004). This model is composed of coupled Euler equations for each phase combined with a volume fraction equation. A typical flow consists of both gaseous and solid particle phases. The conservation equations for the gaseous phase (subscript g) follow for volume fraction α or phase indicator function X, density ρ, velocity u and total Energy E:

$$
\begin{aligned}
\alpha_{gt} + \vec{u}_{\text{int}} \cdot \nabla \alpha_g &= \mathrm{S}_\alpha \\
\left(\alpha_g \rho_g\right)_t + \nabla \cdot \alpha_g \rho_g \vec{u}_g &= S_\rho \\
\left(\alpha_g \rho_g u_{gi}\right)_t + \nabla \cdot \alpha_g \rho_g \vec{u}_g u_{gi} + \left(\alpha_g P_g\right)_{x_i} - P_{\text{int}} \left(\alpha_g\right)_{x_i} &= S_u \\
\left(\alpha_g \rho_g E_g\right)_t + \nabla \cdot \alpha_g \rho_g \vec{u}_g E_g + \nabla \cdot \alpha_g \vec{u}_g P_g - P_{\text{int}} \vec{u}_{\text{int}} \cdot \nabla \alpha_g &= S_{\mathrm{E}}
\end{aligned} \quad (1)
$$

Similar equations exist for the particle (or liquid) phase (subscript p or l). These equations have terms that depend on a mean or phase interface velocity u_{int} and Pressure p_{int} multiplied by the volume fraction gradient. These terms are called the non-conservative or nozzling terms. Here we define the mean velocity and pressure via the following summations

$$
\begin{aligned}
\vec{u}_{\text{int}} &= \sum_{i \in g,p} y_i \vec{u}_i \\
P_{\text{int}} &= \sum_{i \in g,p} \alpha_i P_i
\end{aligned} \quad (2)
$$

where y_i is the mass fraction of a given phase. These mean velocities and pressures are used whenever an explicit model is needed for these quantities. The model presented above is that of Saurel and Abgrall (1999) and is not unique. This differs from the interface model presented by Baer and Nunziato (1986). The second of the two types of models presented here avoids much of the need to explicitly utilize these interface models.

The multiphase relaxation terms S, correspond to the interactions between the phases, such as drag and conduction. The source terms that have been implemented follow:

$$
\begin{aligned}
S_\alpha &= +\frac{\dot{m}}{\rho_g} + \mu (P_g - P_l) \\
S_\rho &= +\dot{m} \\
S_u &= +\dot{m} V_{\text{int},i} + \frac{\alpha_l \rho_l}{\tau_v} \left(u_{li} - u_{gi}\right) \\
S_E &= +\dot{m} E_{\text{int}} + \frac{\alpha_l \rho_l}{\tau_v} \vec{V}_{\text{int}} \cdot \left(\vec{u}_l - \vec{u}_g\right) + \frac{\alpha_l \rho_l C_v}{\tau_c} \left(T_{li} - T_{gi}\right) + \mu P_{\text{int}} (P_g - P_l)
\end{aligned} \quad (3)
$$

where $\dot{m}$ is the chemical production of gas, τ_v and τ_c are drag and conduction time constants, and μ is an inverse compaction stress. The complexities of drag coefficients and Nusselt numbers for conduction have been algebraically folded into the two time constants.

The phase conservation equations have been divided into hydrodynamic and multiphase relaxation terms. The methods presented here treat these equations in an operator split manner between these two types of terms. This yields a two step process where typically the multiphase relaxation terms are evaluated via backward Euler time integration. It is a simple modification to weave a Runge-Kutta time stepping scheme into this system, but this is often at the expense of a final solution that violates a desired mechanical and thermodynamic state. This two-step process has the added attractiveness in that if the hydrodynamic terms are stable and not stiff in the absence of any relaxation terms, then the backward Euler treatment of the relaxation terms will be stable for most combinations of relaxation terms.

The multiphase relaxation processes considered by this model are standard particle conduction and drag formulations that have been averaged to the phase level. Chemistry has also been included. Perhaps the most interesting of these multiphase relaxation processes are the treatments of compaction and pressure relaxation. For cases where the compaction viscosity is unknown, the pressure relaxation model defaults to an infinite relaxation rate or pressure equilibration. Note that pressure equilibration formally makes the multiphase equations ill-posed. However, the fact that the hydrodynamic terms are operator split from the pressure relaxation or compaction terms appears to preserve the well-posedness of the numerical solution.

The hydrodynamic terms have a simplified vector form

$$
\vec{U}_t + \nabla \cdot \vec{F} + \vec{H} = 0 \quad (4)
$$

Where $\vec{U} = \left(\alpha, \alpha\rho, \alpha\rho\vec{u}, \alpha\rho E\right)$ is the state vector, $\vec{F} = \left(1, \alpha\rho\vec{u}, \alpha\rho\vec{u}u_i + \alpha p, \alpha\rho\vec{u}E + \alpha\vec{u}p\right)$ is the conservative flux and $\vec{H} = \left(\vec{u}_{\text{int}} \bullet \nabla\alpha, 0, P_{\text{int}} \nabla\alpha, P_{\text{int}} \vec{u}_{\text{int}} \bullet \nabla\alpha\right)$ is the vector of nozzling terms. The nozzling terms are associated with the accelerations produced by a phase being squeezed by the presence of other phases. The numerical methods described below combine Riemann solvers for a rigorous treatment of the flux vector coupled with compatible treatments of the non-conservative terms. All of the numerical methods described in this abstract exhibit the free-stream preservation property that a multiphase mixture at constant velocity will remain

in mechanical equilibrium. This property is equivalent to the property that a solution with constant u and P will remain constant in u and P even in the presence of volume fraction and density gradients.

Associated with this quasi-conservative formulation (the sum of the phase equations is conservative), is an equivalent set of ``non-conservative" primitive variable equations:

$$\vec{W}_t + A_x \vec{W}_x + A_y \vec{W}_y + A_z \vec{W}_z = 0 \qquad (5)$$

Where $\vec{W} = (\alpha, \rho, u_i, p)$ is the vector of primitive variables and A_{xi} is the primitive variable coefficient matrix for the ith direction:

$$A_{x_i} = \begin{bmatrix} u_{\text{int},i} & 0 & 0 & 0 \\ \frac{\rho}{\alpha}\left(u_i - u_{\text{int},i}\right) & u_i & \rho & 0 \\ \frac{P - P_{\text{int}}}{\alpha\rho} & 0 & u_i & 1/\rho \\ \frac{\rho c^2 \left(u_i - u_{\text{int},i}\right)}{\alpha} & 0 & \rho c^2 & u_i \end{bmatrix} \qquad (6)$$

The primitive equations are used in this model as part of a MUSCL-Hancock predictor-corrector to interpolate the conserved state from zone centers to zone faces and extrapolate this state in time to the middle of the timestep. This extends the time-space accuracy of the methods to second order.

NUMERICAL METHOD

Approximate Riemann Solvers

Although the underlying equations are non-conservative, an approximate Riemann solver formalism is used to formulate the equations. Approximate Riemann solvers have the advantage that only simple estimates of wave speeds are required for the formulation of a stable algorithm. This removes the need to explicit consider the form of the equation of state in the construction of the method. The approximate Riemann solvers in this paper are of two fundamental types: 1) minimum and maximum wave speeds of the entire system of phases are used to construct the fluxes of each individual phase and 2) individual phase speeds are used for the phase fluxes, and the fluxes are appropriately combined to form a method stable from the entire system. The first approach is guaranteed to be stable and monotone. The second approach has the potential to be much more accurate as it requires less diffusion to track each individual phase. However, it is computationally more demanding as it requires multiple combinations of flux evaluations for each phase flux. The Riemann solvers used in this framework are all variants of three fundamental types of single-phase approximate Riemann solvers, Rusanov, HLL, and HLLC. These Riemann solvers are differentiated by the number of characteristics used in the computation of the diffusion needed to upwind the characteristic waves associated with rarefactions, phase contact surfaces, and shocks. Rusanov uses the maximum wave speed, $S^{\max}$ to insure that all waves are adequately upwinded. HLL uses the fastest positive, S^{+} and negative, S^{-} wavespeeds to span the fan of all waves for a lower overall amount of diffusion. HLLC is the most accurate for single phase flow, but the special logic for contact surfaces can be confused by the multiple waves present in multiphase flow.

For simplicity of discussion, all of the methods will be presented in one dimension:

$$U_i^{n+1} = U_i^n - \frac{\Delta t}{\Delta x}\left(F_{i+1/2}^n - F_{i-1/2}^n\right) + \frac{\Delta t}{\Delta x}\left(H_{i,i+1/2}^n - H_{i,i-1/2}^n\right) \qquad (7)$$

This formula is easily extended to multiple dimensions by applying the appropriate divergence and gradient operators. The dual position subscript for the nozzling term H reflects its non-conservative nature. The first subscript denotes the zone it belongs to. The second subscript denotes the face of that zone to which it is attached. Unlike the flux terms, a sum over zones will not cause the nozzling terms to telescopically collapse the sum to a sum of boundary values. Each of the following methods is specified by its own unique numerical flux-nozzling pair.

Multiphase Method of Saurell and Abgrall

The methods presented by Saurell and Abgrall (1999) are the most efficient of the two types of solvers in that each phase is treated independently of the others. The Saurell and Abgrall methods are

based solely on the *u-P* free-stream preservation property. The following flux-nozzling pairs in one dimension are derived by applying a system maximum wavespeed to all phases. The Rusanov pair is given by:

$$F_{i+1/2} = \frac{1}{2}(F_L + F_R) - \frac{S_{\max}}{2}(U_R - U_l) \qquad (8)$$
$$H_{j,i+1/2} = F_j^{lag}(\alpha_i + \alpha_{i+1})/2$$

and the HLL pair by

$$F_{i+1/2} = \frac{S^+F_L - S^-F_R}{S^+ - S^-} - \frac{S^+S^-}{S^+ - S^-}(U_R - U_l) \qquad (9)$$
$$H_{j,i+1/2} = F_j^{lag}\left(\frac{S^+\alpha_L - S^-\alpha_R}{S^+ - S^-}\right)$$

where the "Lagrangian" flux is defined by

$$F_j^{lag} = \left(u_{\text{int},j}, 0, P_{\text{int},j}, u_{\text{int},j}P_{\text{int},j}\right) \qquad (10)$$

It was found that these flux-nozzling pairs require very small initial timesteps in the presence of very strong pressure gradients coupled with strong volume fraction gradients. The initial timestep can be greatly increased once the volume fraction gradient has been sufficiently diffused. A new modification of the nozzling terms eliminates this timestep restriction. The corrected nozzling term for Rusanov is:

$$\begin{aligned} H_{j,i+1/2} &= \hat{F}_j^{lag}\left(\hat{\alpha}_{i+1/2} - \alpha_j\right) \\ \hat{F}_j^{lag} &= \left(u_{\text{int},j}, 0, \hat{P}_{\text{int},j}, U_{\text{int},j}\hat{P}_{\text{int},j}\right) \\ \hat{P}_j^{lag} &= \frac{\alpha_L P_L + \alpha_R P_R}{\alpha_L + \alpha_R} \\ \hat{\alpha}_{i+1/2} &= \frac{\alpha_L + \alpha_R}{2} \end{aligned} \qquad (11)$$

and for HLL is:

$$\begin{aligned} H_{j,i+1/2} &= \hat{F}_j^{lag}\left(\hat{\alpha}_{i+1/2} - \alpha_j\right) \\ \hat{F}_j^{lag} &= \left(u_{\text{int},j}, 0, \hat{P}_{\text{int},j}, U_{\text{int},j}\hat{P}_{\text{int},j}\right) \\ \hat{P}_j^{lag} &= \frac{S^+\alpha_L P_L - S^-\alpha_R P_R}{S^+\alpha_L - S^-\alpha_R} \\ \hat{\alpha}_{i+1/2} &= \frac{S^+\alpha_L - S^-\alpha_R}{S^+ - S^-} \end{aligned} \qquad (12)$$

This reinterpretation of the nozzling terms uses integration by parts to avoid overly driving a phase with little mass by a flux from a nearby zone with much more mass. This new nozzling term is appropriately normalized to insure that the sum over all phases is zero.

One of the defects of this model is that it requires an explicit usage of the interface velocities and pressures.

Multiphase Method of Chinnayya

This method is fundamentally paired with the HLLC Riemann solver as it requires an estimate of the various material contact-surface velocities at zone faces. This method uses the volume fraction as an indicator function, *X*, to apportion the contacts between phases. Each contact in this collection of contact surfaces is processed by a single phase HLLC Riemann solver to determine its evolution and hence the flux and nozzling needed by each phase. Further information on this Riemann solver is found in the excellent articles by Abgrall and Saurell (2003) and Chinnayya et Al. (2004). The flux-nozzling pair for this method follows:

$$\begin{aligned} F_{i+1/2}(k) &= \sum_j S_{kl} X^*_{i+1/2}(k,l) F^*_{o+1/2}(k,l) \\ H_{j,i+1/2} &= \sum_{j \neq i} S_{kl}\left[X^*_i\right](k,l) F^{lag}_{o+1/2}(k,l) \\ F^{lag}_{i+1/2}(k,l) &= \left(u^*_{kl}, 0, p^*_{kl}, p^*_{kl}u^*_{kl}\right) \end{aligned} \qquad (13)$$

Where $F^*_{i+1/2}(k,l)$ is the flux computed from the single phase HLLC solver with pure phase *k* on the left and phase *l* on the right. The quantities u^*_{kl} and p^*_{kl} are the contact velocities and pressures derived from the HLLC solver. The indicator function S_{kl} is unity in the presence of a *k-l* contact and zero elsewhere. $\left[X^*_{j,i+1/2}\right]$ is the jump in *X* associated with a contact. While this method is potentially much more accurate, it is computationally more demanding. The method requires that the flux for each phase is the sum of combinations from all possible contacts between this phase and all the others. The processing of each contact requires up to 4 HLLC evaluations, each of which has an HLL evaluation embedded inside it for processing the contact phase speed.

The cost of this algorithm is greatly offset by its ability to avoid two fundamental problems of the Saurell and Abgrall (1999) methods: the elimination of the need for system maximum wave speeds and the ability to avoid specifying interface velocities and pressures. The Chinnayya model implicitly calculates mean interface velocities and

pressures via the HLLC flux evaluations. Another attraction of this algorithm is that it is a logical endpoint in the evolution of the Saurell and Abgrall fluxes. The correction that removed the initial timestep restriction is very analogous to replacing the average volume fraction in the nozzling terms by a more appropriate jump condition in volume fraction.

MUSCL-Hancock predictor-corrector

This multiphase framework uses the same predictor for both types of Riemann solvers as part of a predictor-corrector method to achieve formal second-order accuracy, In isolation, each Riemann solver is inherently first-order, as they at most first-order upwind a desired collection of characteristics. The sole reason for comparing different Riemann solvers is to determine the effect of accurately incorporating more waves into the solution and hence minimize the amount of diffusion required to stably integrate the multiphase equations. The predictor used here for all three methods is the standard MUSCL-Hancock approach by which the primitive equations are used to predict left and right states $\left(\vec{W}_L, \vec{W}_R\right)$ about each computational face. The conservation properties for each phase are then enforced by converting the primitive vector of edge states $\left(\vec{W}_L, \vec{W}_R\right)$ to the conserved edge vectors $\left(\vec{U}_L, \vec{U}_R\right)$ and evaluating the Riemann solver with these conserved quantities. Explicit details of the MUSCL-Hancock approach are described in Toro (1999).

The chief drawback of using a common predictor for all three approximate Riemann solvers is the reintroduction of the interface velocity and pressure model for the HLLC method.

This drawback is offset by a couple of mitigating factors. The only ghost zone evaluation and hence parallel communication is that required by the MUSCL predictor for computing left and right states at the faces of computational zones. Another offset is the single phase nature of the monotonic slopes used by the predictor. The original Chinnayya algorithm uses the Riemann solver as a predictor followed by monotonic interpolation to faces for left and right states. This Riemann solver is then reused using these new left and right states. Unfortunately, the quantity independent slope limiting used by the interpolation eliminates the state interdependencies that the HLLC based Riemann solver seeks to preserve.

It should be noted that for stability the Chinnayya model requires additional nozzling terms in the corrector associated with an internally present contact.

RESULTS

Water-Air Shock Tube

A useful test problem for method comparison is the following water-air shock tube. This test problem is present in both Chinnayya (2004) and Saurell and Abgrall (1999) and is more fully described in these two papers. This problem is a stiff test of multiphase numerical methods consisting of a 1 Gpa water region expanding into a 5 Mpa air region. While lower than typical detonation pressures, this test problem presents a canonical single phase shock tube of interest with relevant density and pressure gradients. This is an example of a densely loaded multiphase flow problem. This simulation was done with a very small drag relaxation time scale $(\tau_v = 1.e-20)$ and solutions were compared after an integration period of 229 microseconds.

All of the flux-nozzling pairs are viable methods for this problem. Below is a comparison of the mean barycentric density for four predictor-corrector combinations. It was found that the largest effect on solution accuracy for this problem was the presence of a predictor. This is probably due to the fact that the characteristic represented by the water shock is by far the largest in magnitude and obviates the need for a sophisticated evaluation of the other waves involved. The predictor is able to minimize overall dissipation by limiting the diffusion from the Riemann solver to only a small region around the water shock.

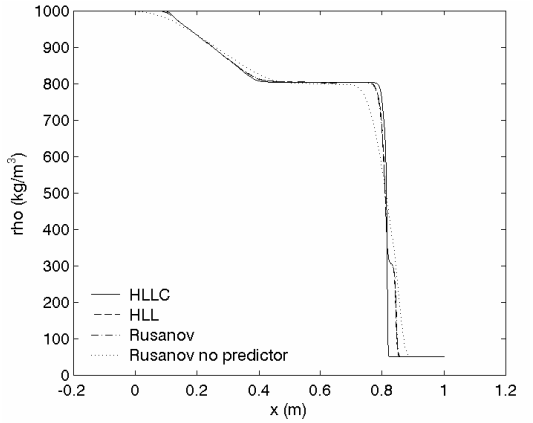

FIGURE1: Density Comparison.

Particle Dispersion

Zhang and Frost's particle dispersion experiments are a very useful dataset for validating multiphase flow models. This is an example of a multiphase flow that transitions from a densely loaded detonation problem to the dilute flow limit within less than five charge radii.

Their experiments consisted of spherical charges of nitromethane with 0.6 by volume fraction loading of steel spherical particles of various sizes. A unique feature of their observations is that steel particles with sufficient mass can easily penetrate the explosively driven shock front into the quiescent air.

Below are graphed the simulated and experimentally derived particle and shock fronts for their 11.8 cm diameter charge with 473 micron steel particles. Again all of the methods are producing credible simulations. The different methods do exhibit different behaviors which are magnified in the particle phase. This test problem, more than the water-air shock tube, effectively shows off the additional physics that have been incorporated into the HLLC based Riemann solver. The wavespeed associated with the shock front is an inappropriate wavespeed for the bulk of the problem. The particle front is really a contact surface. The Rusanov and HLL approaches, which use system maximum wave speeds, appear to have particle fronts that are excessively slowed as compared to the HLLC particle fronts.

A further drawback of the system based approaches is their inflexibility in incorporating the effects of changing volume fraction in controlling their dissipation. As the particle transitions from the charge to the surrounding air, the particle phase volume fraction falls off very sharply as a function of distance. Hence, a system maximum wavespeed approach, which takes into account the steel shock Hugoniot, is dramatically over damping the air shock behavior even though the steel volume fraction may only be a small fraction of a percent.

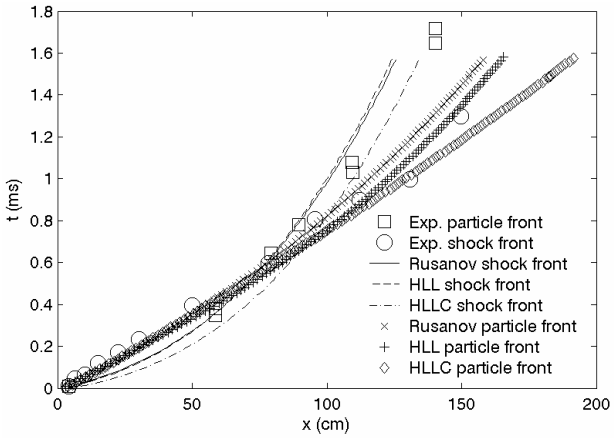

FIGURE 2: Comparison of Particle and shock fronts.

CONCLUSIONS

We have presented a predictor-corrector model that combines modifications to the original Saurell Abgrall and Chinnayya algorithms that increases their efficiency and stability. These modifications are used to simulate two energetic test problems. The first is a single-phase, but multi-material analog of an exploding medium. The second problem transitions from a 20 Gpa detonation to a 0.4 Mpa air shock within the space of 2 meters. The particle loading transitions from 60 percent by volume to small fractions of a percent in less than five charge radii.

These results have encouraged the application of this model to additional non-ideal behavior such as DDT (Deflagration to Detonation Transition) and other non-ideal explosives.

ACKNOWLEDGEMENTS

This work was performed under the auspices of the U.S. Department of Energy by the University of California, Lawrence Livermore National Laboratory under contract No. W-7405-Eng-48.

This work was also supported by the Joint DoE/DoD Munitions Program and the DoD HPC office.

REFERENCES

1. Baer and Nunziato, “A two-phase mixture theory for the deflagration-to-detonation transition (DDT) in reactive granular materials”, *Inter. J. Multiphase Flow*, Vol. 12, pp 861-889.

2. Chinnayya, A., Daniel, E., and Saurel, R., “Modeling detonation waves in heterogeneous energetic media”, *J. Comput. Phys*, Vol. 196, pp 490-538, 2004.

3. Toro, E. F., “Riemann Solvers and Numerical Methods for Fluid Dynamics”, Springer-Verlag, New York, 1999.

4. Saurel, R., and Abgrall, R., “A Multiphase Godunov Method for Compressible Multifluid and Multiphase Flows”, *J. Comput. Phys*.,Vol 150, pp 425-467, 1999.

5. Zhang, F., Frost, D. L., Thitouk, P. A., and Murray, S. B., “Explosive Dispersal of solid particles”, *Shock Waves*, Vol. 10, pp. 421-442, 2001.